Monoenergetic Electronic Beam Production Using Dual Collinear Laser Pulses

A. G. R. Thomas,[1] C. D. Murphy,[1,2,*] S. P. D. Mangles,[1] A. E. Dangor,[1] P. Foster,[2] J. G. Gallacher,[3] D. A. Jaroszynski,[3] C. Kamperidis,[1] K. L. Lancaster,[2] P. A. Norreys,[2] R. Viskup,[3] K. Krushelnick,[1,†] and Z. Najmudin[1]

[1]*Blackett Laboratory, Imperial College London SW7 2BZ, United Kingdom*
[2]*Central Laser Facility, Rutherford Appleton Laboratory, Oxon OX11 0QX, United Kingdom*
[3]*Department of Physics, University of Strathclyde, Glasgow G4 0NG, United Kingdom*

(Received 24 December 2007; published 24 June 2008)

The production of monoenergetic electron beams by two copropagating ultrashort laser pulses is investigated both by experiment and using particle-in-cell simulations. By proper timing between guiding and driver pulses, a high-amplitude plasma wave is generated and sustained for longer than is possible with either of the laser pulses individually, due to plasma waveguiding of the driver by the guiding pulse. The growth of the plasma wave is inferred by the measurement of monoenergetic electron beams with low divergence that are not measured by using either of the pulses individually. This scheme can be easily implemented and may allow more control of the interaction than is available to the single pulse scheme.

DOI: 10.1103/PhysRevLett.100.255002 PACS numbers: 52.38.Kd, 41.75.Jv

The laser wakefield accelerator (LWFA) [1] uses a high-intensity laser pulse to generate an electron plasma wave, with relativistic phase velocity, oscillating at the electron plasma frequency, $\omega_p = \sqrt{e^2 n_e / m_e \epsilon_0}$, where n_e is the local electron number density. Electrons that are not part of the relativistic fluid can be trapped in the wave, under certain conditions, and accelerated.

It is hoped that electron beams from LWFAs will eventually provide sources of relativistic electron beams and x rays for applications such as chemical and biological spectroscopy, medical imaging, and radiation therapy. If viable, they are expected to revolutionize such sources, making them available at lower cost to small scale facilities such as universities or hospitals.

With advances in laser technologies, pulses of duration close to the plasma period ($\tau_p = 2\pi/\omega_p$) can now be generated directly. It was previously suggested that a high-amplitude wakefield could be generated by multiple suitably spaced short pulses [2]; if subsequent laser pulses are timed to push the electrons in their direction of motion as they overshoot their equilibrium position, then the plasma wave amplitude can grow resonantly. However, as pulse length reduction has been accompanied by an increase in the power of the short pulses, multiple pulses have been deemed to be unnecessary since it is now possible to grow large amplitude plasma waves with a single intense ultrashort laser pulse.

These high-amplitude waves can be a source for the trapped electrons by self-injection from the plasma itself. This occurs in three dimensions when the accelerating phase of the electric field reaches sufficient amplitude to prevent electrons from slipping into a decelerating phase of the wake [3]. In recent experiments [4–6], it has been demonstrated that a single pulse injection process can produce electron beams of narrow energy spread and small divergence, but requires >10TW, <100 fs laser systems, which are by no means ubiquitous. In addition, since the propagation of a pulse with $I\lambda^2 > 10^{19}$ W cm^{-2} required for self-injection is dominated by modulational effects, a higher degree of complexity may be required to control the interaction.

Alternative means of injecting electrons by the influence of secondary laser beams have also been previously suggested [7–9]. These include a scheme whereby counterpropagating laser pulses have been shown to offer control of some of the properties of the electron beam [10]. In addition, optical guiding of a pulse in a gas-filled capillary discharge has been demonstrated to lower the pulse power requirement for producing high-energy electron beams [11].

Presented in this Letter is the first evidence for production of monoenergetic electron beams generated by the interaction of two copropagating ultrashort laser pulses. Note that although collinear pulses were used in [12,13], in those experiments the resulting spectrum was not monoenergetic and the mechanism was different. Here, a laser pulse with a large focal spot (large f number) was used to generate a low amplitude plasma wave. This was then used as a guiding structure for a tightly focused (low f number) pulse. Particle-in-cell simulations of the experiment show that the tightly focused pulse was guided at a smaller spot size than the guiding pulse, for much longer than its Rayleigh range, if correctly phased within the wakefield [14]. Electrons, produced when the low f-number pulse focused, were accelerated in the quasistatic fields of the wakefield, resulting in monoenergetic beams.

The experiments were carried out on the 600 mJ arm of the $\tau_L = 40 \pm 5$ fs full-width half-maximum (FWHM) Ti:sapphire ASTRA laser operating at wavelength $\lambda_0 =$ 800 nm. A thin (5 mm) beam splitter was used to produce two $E_{\text{pulse}} = 300$ mJ pulses that were focused using $f/3$ and $f/16$ off-axis parabolic mirrors collinearly, and with parallel polarization, into helium gas from a 2 mm diameter supersonic gas nozzle (Fig. 1). On ionization by the

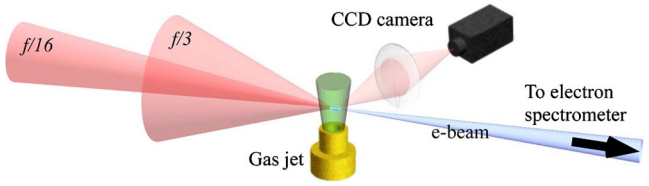

FIG. 1 (color online). Schematic of the experimental setup.

leading edge of the laser, a plasma of electron number density $n_e = 1 \times 10^{19}$ cm^{-3} was produced. This density was chosen so that the pulse with $f/16$ focusing did not produce a measurable electron signal, but so that electrons were detected using $f/3$ focusing.

The FWHM spot sizes for the pulses focused by the $f/3$ and $f/16$ optics were 5 μm and 25 μm, respectively. This resulted in focused intensities of 1.9×10^{19} W cm^{-2} and 0.8×10^{18} W cm^{-2} corresponding to normalized vector potentials a_0 of 3 and 0.6. In both cases, the longer focal length pulse passed through the beam splitter, for which a 5 fs increase in pulse length was measured. A motorized timing slide allowed control of the longitudinal spacing of the two pulses. The pulses could be overlapped to an accuracy of about one focal spot size (i.e., $\sim$25 μm), and were limited by the mechanical stability of the laser pointing at the time.

The timing slide path length was measured to ± 1 μm (± 3.3 fs) accuracy. This accuracy was limited by the measured relative timing of the two pulses Δt, which was done by maximizing the plasma defocusing of one pulse by the other, at a fraction of a percent of full power. The error in this method was therefore of the order 40 fs (i.e., $\sim \tau_L$). The energy spectrum of the accelerated electrons was obtained using a magnetic spectrometer with image plates as the detector, as in [4]. The acceptance cone of the electron spectrometer was $f/200$. Light emitted from the interaction was reimaged orthogonally to the beam axis, to discern the propagation of the laser.

Using the pulse with $f/16$ focusing—henceforth referred to as the guiding pulse—alone resulted in no measurable electron signal above noise level at the chosen density. The pulse with $f/3$ focusing—henceforth referred to as the drive pulse—would consistently produce electron bunches of a few pC charge, but these had a large divergence and the energy spectrum was best described by a single temperature fit.

Using both pulses, the spectra obtained were non-Maxwellian with obvious structure [Figs. 2(a)–2(c)]. Indeed, on many of the shots, the Maxwellian spectra that the drive pulse alone produced were almost completely suppressed, with the majority of recorded electrons in a single low energy spread beam. For example, the beam shown in Fig. 2(c) had an energy spread $\Delta E = 0.6$ MeV (FWHM). This monoenergetic beam was also very well collimated, with an angular divergence often less than the opening angle of the collimator, 2×10^{-5} steradians solid angle

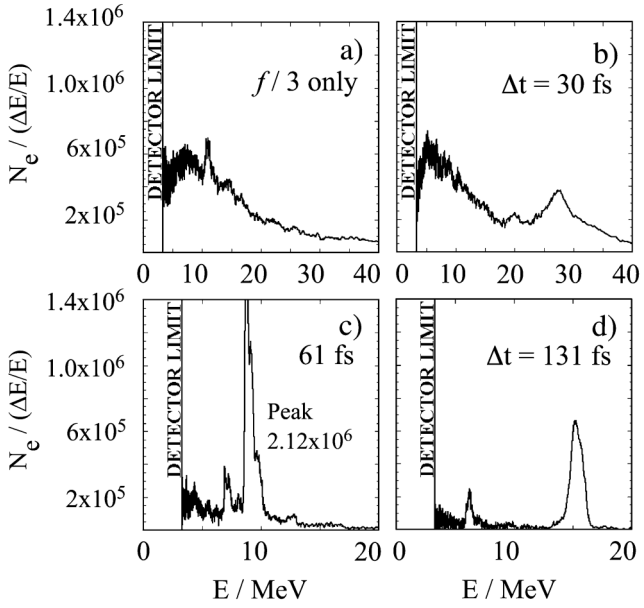

FIG. 2. (a) Typical electron spectra with the drive pulse only, (b)–(d) quasimonoenergetic electron spectra with highest charge shown for various timings between the drive and guiding laser pulses. $n_e = 1 \times 10^{19}$ cm^{-3} and $E_{\text{pulse}} < 300$ mJ.

or 2.5 mrad half-opening angle, the smallest being 5×10^{-6} steradians.

The total charge as a function of the timing between the beams, Δt, has a maximum at $\Delta t = 30$ fs, which is likely to be the timing when the pulses were overlapped sufficiently to act as a single pulse with double the energy, since it is within the error by which $\Delta t = 0$ was set. The relative mean energies, $\bar{W}_R$, in the spectrum are plotted for all shots in the data set in Fig. 3, including nonmonoenergetic spectra. The mean energy $\bar{W} = \int_0^\infty W dN(W) / \int_0^\infty dN(W)$. $\bar{W}_R = \bar{W} - \min(\bar{W})$.

From Fig. 3(a), it is evident that there was an enhancement in the mean energy over a range of timings, from when the pulses are overlapped, to when the guiding pulse leads the driver by a few plasma periods ($\approx$6). This indicates the extent of the coherent plasma wave structure at this density. Note that because of the low intensity of the guiding pulse, a single wave period was not expected as in [15]. The decay of the energy enhancement indicates the eventual damping of the coherent plasma wave due to, e.g., radial anharmonicity [16].

Figure 3(b) shows $\bar{W}_R$ averaged over clusters of shots taken at the same time (i.e., without moving the timing slide between shots). For guiding of the drive pulse in the plasma wave generated by the guiding pulse, we might expect a variation of the weighted energy with a period of $2\pi/\omega_p \approx 33$ fs, and the data do indeed show large changes in the observed energy for small changes in the pulse timings. Periodic behavior is expected due to the underlying plasma wave structure, but the data are not sufficient to give an exact period to this oscillation. This is because the laser pulses were slightly longer than the

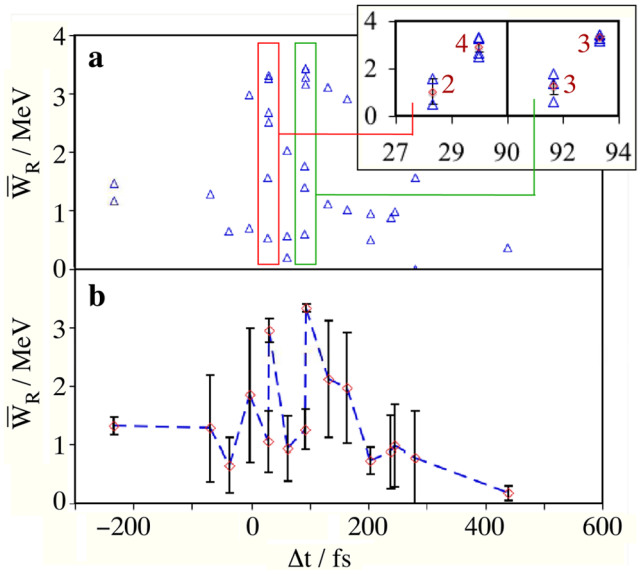

FIG. 3 (color online). (a) Relative mean energy $\bar{W}_R$ as a function of the relative arrival time between the pulses (Δt), and (b) $\bar{W}_R$ averaged over clusters of shots taken at the same time. The black bars show the standard error in these shots. The inset of (a) shows expanded versions of the highlighted regions, showing the relative stability of $\bar{W}_R$ for certain timings, where the number labels indicate the number of shots in the cluster.

plasma period, combined with experimental errors in relative timing and, most importantly, laser pointing. It is worth emphasizing that there are some specific timings that exhibit both enhanced electron energy and reduced shot-to-shot fluctuations in the beam energy. These are likely to be timings when the drive pulse was well phased in the guiding wakefield.

Side-scattered radiation of the guiding pulse by itself, imaged in the direction transverse to propagation, was not measurable above noise level. With the drive pulse alone, the extent of the emission was ~ 10 μm, which is comparable to the Rayleigh range of this pulse. However, when the drive pulse overlapped the guiding pulse, an extended emission region on the order of 1 mm was observed, which is longer than the Rayleigh range of the driver pulse. These shots correspond to the cluster of 4 shots in the inset of Fig. 3(a). The 2 shots with lower $\bar{W}_R$ do not show the extended emission despite being separated by $\ll \tau_L$.

An extensive series of two-dimensional particle-in-cell simulations were run using the code OSIRIS [17]. These were run under similar parameters to the experiments and for a large number of relative arrival times, Δt, between the pulses. Because of computational constraints, Δt could not be longer than a few plasma periods; however, the control of the timing within that range was obviously much higher than in the experiment.

The simulations clearly indicate the presence of plasma waveguiding [14] of the tightly focused pulse. This counteracted the filamentary behavior of the tightly focused pulse [18] and extended its propagation as a single filament. There is a strong phase dependence to this effect in these simulations arising as a result of the fine control of Δt. Plasma waveguiding relies on the guided pulse being in a predominantly focusing refractive index structure. Since a plasma wave is periodically focusing and defocusing it is evident that for certain Δt the pulse will be guided and for a $\pi/2$ phase shift the pulse will be defocused.

For simulations when the drive pulse was in phase with the plasma wave created by the guiding pulse, it was focused by the density depression and its propagation dictated by the guiding pulse. In addition, the two wakefields were in phase, which produced a larger amplitude wake than either pulse alone. When the driver pulse was out of phase with the wave bucket, the density structure acted to defocus the pulse. This guiding and defocusing is shown in Fig. 4. Figure 4(a) shows the situation when the drive pulse phase was well phased within the guiding wake, and hence a large fraction of the pulse energy was trapped in a single stable filament. In Fig. 4(b), the wake of the drive pulse was not well phased in the guiding structure. The drive pulse was mainly defocused with only a fraction of laser energy trapped, 62% of Fig. 4(a).

In Fig. 5, time histories of the intensity profiles of (a) the unguided drive pulse, (b) the guided drive pulse, and (c) the guide pulse are shown as they propagated through the plasma. The guided drive pulse (b) was in phase with the wake, and was clearly guided over a distance longer than its Rayleigh length ($z_R = 33$ μm). The nonideal pulse lengths (similar to those of the experiment) meant that not all of the driver was within the focusing phase of the plasma wave, and hence some of the pulse energy dif-

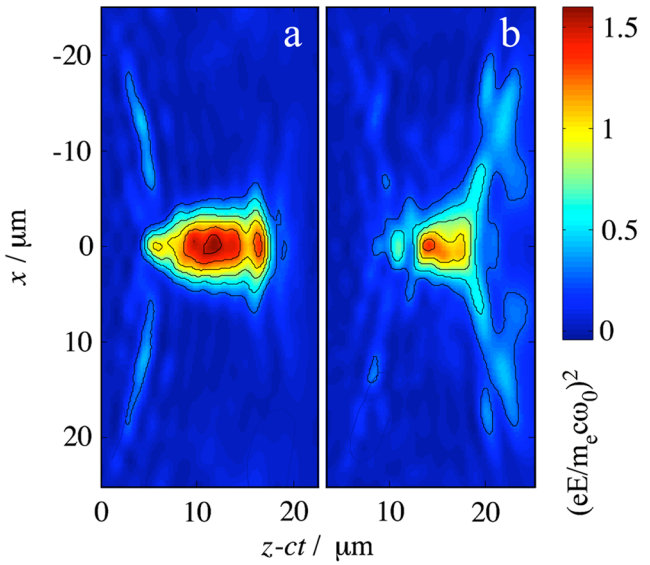

FIG. 4 (color online). The normalized intensity $e^2E_0^2/m^2c^2\omega_0^2$ of driver pulses having propagated 1500 μm in a density of $n_e = 1 \times 10^{19}$ cm^{-3} with a separation of (a) 21 μm (well phased) and (b) 18 μm (not well phased). Contours are given at intervals of 0.25. The energy trapped in filament (b) is 62% of (a).

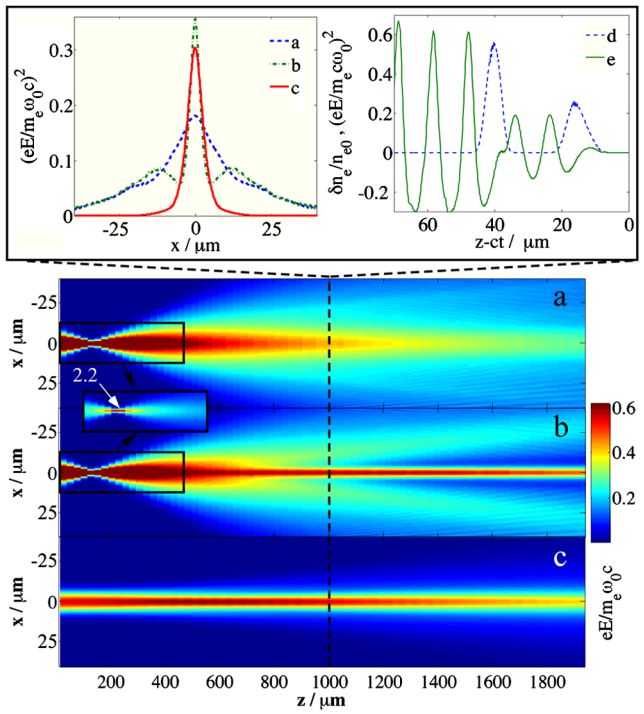

FIG. 5 (color online). The transverse envelope as a function of propagation distance (a) driver without a guide pulse and (b) driver with appropriately timed guide pulse. (c) The transverse envelope of the guide pulse only for comparison. The transverse envelope was found by integrating the electric field of the pulse longitudinally (z). The graphs show (left) the intensity profiles in the transverse (x) direction and (right) the wakefield and pulse profiles along the axis of propagation. (d) The laser envelope, and (e) $\delta n_e/n_{e0}$ for the wake.

fracted away. However, the majority of the pulse energy was trapped in a single filament.

The inset graphs to Fig. 5 show the intensity profiles for the pulses and wake density profile after 1.05 mm propagation. A Gaussian fit to the temporally averaged central filaments gives a *full* width at $1/e^2$, $2w$ for each of the pulses. The guide pulse (c), was very close to λ_p in spot size, $2w = 9.0\ \mu$m, as is expected for a self-guided short pulse with $P \sim P_{\mathrm{crit}}$ [18,19]. For the unguided driver pulse (a), the spot size was $2w = 20.8\ \mu$m and has significant wings, whereas for the guided driver pulse (b), the spot size was $2w = 5.6\ \mu$m.

Earlier in the interaction [(a) and (b), inset boxes], the drive pulse focused to high intensity and trapped an electron bunch. After defocusing, electron trapping ceased, and the behavior was strongly influenced by the presence of the guide pulse. In the unguided case, the lack of quasistatic wakefields maintained for a long propagation length resulted in a broadening of the electron spectra; cf. [18]. However, in the guided case, the electron bunch was accelerated in a quasistatic wakefield, resonantly generated by the two pulses for a relatively long time, and therefore remained monoenergetic. This means the electron trapping can be controlled through the focusing of the drive pulse.

In summary, under the right conditions of overlap and timing between two collinear laser pulses, electron beams of high quality, both in terms of energy spread and divergence, were produced. By improving the laser pulse characteristics, particularly the pulse power and pointing, the electron beam stability should be enhanced. In addition, for higher laser powers, the energy split between the two pulses need not be 50/50; less energy may be put into the guiding pulse. Through controlling the propagation of a tightly focused driver pulse, this scheme should offer the ability to control monoenergetic electron beam production and is easy to implement. Consequently, this scheme may be of interest in the development of compact sources of energetic electron beams.

This work was supported by EPSRC and Alpha-X. The authors also gratefully acknowledge the OSIRIS consortium (UCLA/IST Lisboa/USC) for the use of OSIRIS.

*Present address: The Ohio State University, Columbus, OH 43210, USA.

†Present address: The University of Michigan, Ann Arbor, MI 48109, USA.

[1] T. Tajima and J. M. Dawson, Phys. Rev. Lett. **43**, 267 (1979).
[2] D. Umstadter, E. Esarey, and J. Kim, Phys. Rev. Lett. **72**, 1224 (1994).
[3] S. Gordienko and A. Pukhov, Phys. Plasmas **12**, 043109 (2005).
[4] S. P. D. Mangles *et al.*, Nature (London) **431**, 535 (2004).
[5] C. G. R. Geddes *et al.*, Nature (London) **431**, 538 (2004).
[6] J. Faure *et al.*, Nature (London) **431**, 541 (2004).
[7] D. Umstadter, J. K. Kim, and E. S. Dodd, Phys. Rev. Lett. **76**, 2073 (1996).
[8] E. Esarey, R. F. Hubbard, W. P. Leemans, A. Ting, and P. Sprangle, Phys. Rev. Lett., **79**, 2682 (1997).
[9] C. B. Schroeder, P. B. Lee, J. S. Wurtele, E. Esarey, and W. P. Leemans, Phys. Rev. E **59**, 6037 (1999).
[10] J. Faure *et al.*, Nature (London) **444**, 737 (2006).
[11] W. P. Leemans *et al.*, Nature Phys. **2**, 696 (2006).
[12] D. F. Gordon *et al.*, Phys. Rev. E **71**, 026404 (2005).
[13] W.-T. Chen *et al.*, Phys. Rev. Lett. **92**, 075003 (2004).
[14] P. Sprangle, E. Esarey, and A. Ting, Phys. Rev. A **41**, 4463 (1990); P. Sprangle, E. Esarey, and A. Ting, Phys. Rev. Lett. **64**, 2011 (1990).
[15] A. Pukhov and J. Meyer-ter-Vehn, Appl. Phys. B **74**, 355 (2002).
[16] J. M. Dawson, Phys. Rev. **113**, 383 (1959); J.-R. Marquès *et al.*, Phys. Rev. Lett. **78**, 3463 (1997).
[17] R. A. Fonseca *et al.*, in Computational Science-Iccs 2002, Pt Iii, Proceedings (2002), Vol. 2331, pp. 342–351.
[18] A. G. R. Thomas *et al.*, Phys. Rev. Lett. **98**, 095004 (2007).
[19] W. Lu *et al.*, Phys. Plasmas **13**, 056709 (2006).